Note on Efflux from Solid-Gas Fluidized Beds

LEOPOLDO MASSIMILLA and GENNARO VOLPICELLI

Istituto di Chimica Industriale, Universita di Napoli, Naples, Italy

The results of an investigation on outflow of solid and gas through orifices open in the side of fluidized beds have been given in a previous paper (2). The diameter of orifices tested ranged between 3 and 7 mm. These experiments outlined the following features of solid and gas outflow from fluidized beds: flow rates of solid and gas effluxed were almost constant in the range of the flow rate of fluidizing air, separation of solid particles from solid-gas suspension in the column took place immediately upstream of the outflow orifice, and for a given material the ratio Q_A/Q_S decreased as the orifice diameter increased. Experimental results were interpreted by considering the interdependent phenomena: the motion of the gas filtering through the particles and the drag of the solid caused by the filtering air. These phenomena have also been considered by Stockel in his study on high speed flow of fluidized solids in changing area sections (4).

Recently investigation on outflow from fluidized beds has been extended (5). Orifices up to 20 mm. in diameter were tested with silica sand, iron sand, and granulated limestone. The results of these additional experiments and new information on related subjects (3, 4, 6) allow a better insight into the outflow processes from solid-gas fluidized beds.

In previous work equations

$$\frac{Q_A - Q_S}{\left(\dfrac{g_c \Phi D_p \Delta p}{\rho_A}\right)^{0.5}} = 1.54\, r_o^{1.5} \quad (1)$$

and

$$\frac{Q_A}{Q_S} = 1 + \sqrt{\frac{3\, w_p\, \rho_p}{C_D\, \rho_A\, s_p\, r_o}} \quad (2)$$

were developed from energy balance and drag equations according to different hypotheses. Equation (1) was obtained from the assumption that most of the potential energy of the gas was lost owing to friction by the effluent. Equation (2) was derived by equating the drag and inertial forces acting on the particles. Frictional forces between the particles themselves and between the particles and the edge of the orifice were disregarded.

Actually the first hypothesis is more likely, when one considers that kinetic energy of the effluxing solid-gas system was about 10% of the potential energy of the gas upstream orifice. However a fair agreement was found between curves Q_A/Q_S vs. r_o calculated by means of Equation (2) and curves obtained by experimental data, at least for orifices of 5- and 7-mm. diameter. This agreement could depend on an underestimation of drag coefficient. Because of lack of more suitable data the drag coefficient for effluxing particles was obtained by multiplying the drag coefficient for single sphere by a factor about equal to 2. This factor was determined by a broad extrapolation of the formula proposed by Ladenburg for spheres falling in tubes. Rowe (3) has demonstrated that drag coefficient related to the motion of a group of spheres can be one order of magnitude greater than the drag coefficient for single sphere. A higher value of C_D in Equation (2) would considerably lower theoretical ratios Q_A/Q_S with respect to experimental ones. For a true agreement it would be necessary to give full consideration to the effect of interparticle frictional forces.

It should be pointed out that the ratio of particle diameter over orifice diameter has a considerable effect on frictional resistances in outflow of solid from fluidized beds. The higher $D_p/2r_o$ is, the higher the discrepancy between experimental and calculated Q_A/Q_S is. Zenz (6) has interpreted the influence of $D_p/2r_o$ on solid outflow from fluidized beds by extending Brown's concept (1) of solid stagnation on the edge of orifice valid for gravity flow of bulk solid. He succeeded in correlating data of solid ef-

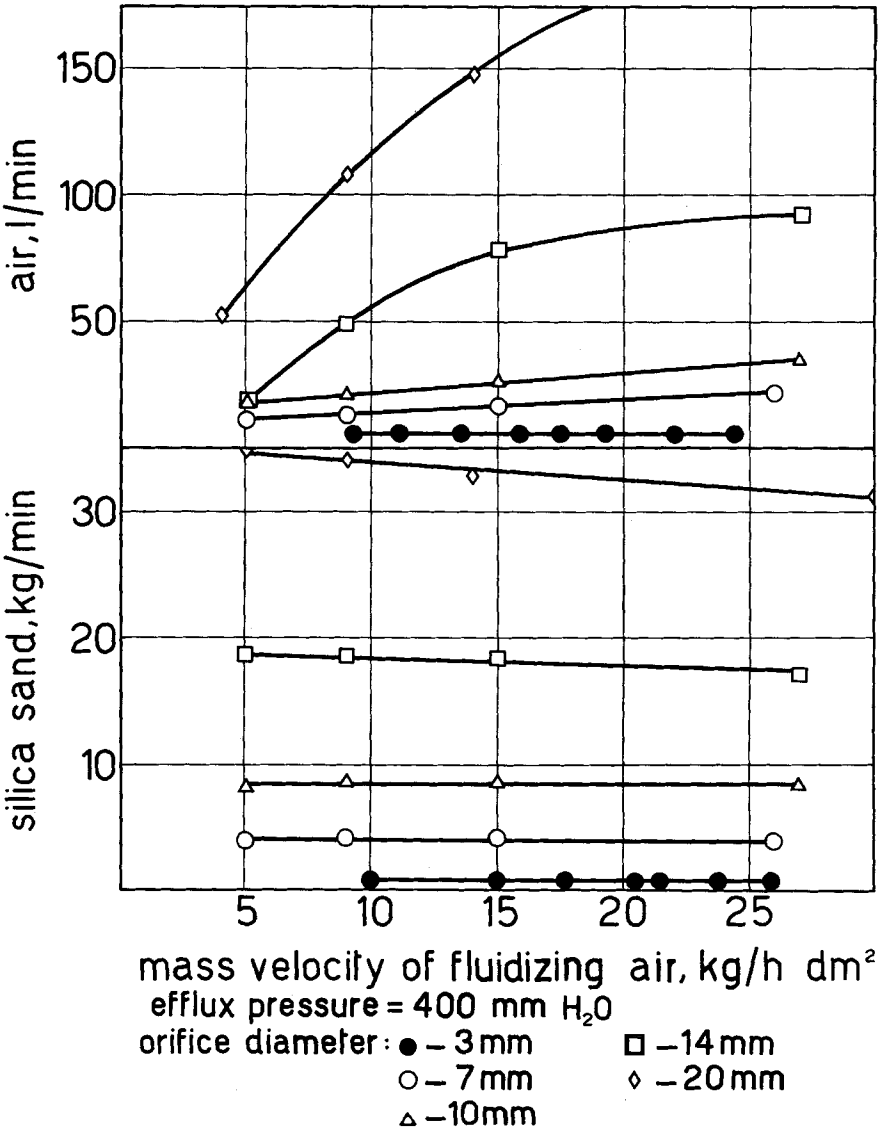

Fig. 1. Flow rate of silica sand and air from orifice as a function of the mass velocity of fluidizing gas. The air flow rate has been measured at atmospheric pressure and at 20°C.

(*Continued from page 138*)

INFORMATION RETRIEVAL

Key Words: Naphthalene-1, Temperature-1, Air-5, Wind Tunnel-5, Spheroid Shape-6, Spheroid Eccentricity-6, Reynolds Number-6, Air Velocity-6, Mass Transfer Rate-7, 8, Sublimation Rate-7, 8, Continuous Phase Mass Transfer Coefficient-7, 8, Extraction-7, 8, Heated Air-10, Wind Tunnel-10.

Abstract: To obtain information on the effect of eccentricity on mass transfer naphthalene spheroids covering a range of eccentricities from 1:1 to 3:1 and having major axes of 1 in. were suspended in a low turbulence, intensity air stream maintained at a constant temperature of about 50°C. Rates of sublimation were obtained over a range of the Reynolds number from 130 to 6,000, the Schmidt number having an approximate value of 2.44. The experimental data from 102 runs were correlated with an estimated standard deviation of 2.1%.

Reference: Skelland, A. H. P., and A. R. H. Cornish, **A.I.Ch.E. Journal, 9,** No. 1. p. 73 (January, 1963).

Key Words: Rates-8, Reactors-9, Monomolecular Reactions-9, Time-6, Rate Constants-10, Matrix Algebra-10, Prediction-8, Conversion-9, Yield-9, Residence-9, Optimization-10, Eigenvalues-10, Straight Line Reaction Paths-10.

Abstract: Many chemical reaction systems of interest to chemical engineers can be closely approximated by first-order or pseudo first-order reactions. The integral solutions can be expressed in matrix notations that are relatively easy to manipulate. The matrix notations are related to straight line reaction paths, quantities that are directly measurable.

Reference: Wei, James, and Charles D. Prater, **A.I.Ch.E. Journal, 9,** No. 1, p. 77 (January, 1963).

Key Words: Pressure Drops-8, Friction Factors-7, Modified Reynolds Number-6, Packed Beds-8, Distended Beds-8, Spheres-8, Wind Tunnel-5.

Abstract: Pressure drops of air flowing through packed and distended beds having five layers of smooth plastic spheres were measured for modified Reynolds numbers between 2,550 and 64,900. A single relationship resulted for both types of beds between the friction factor and the modified Reynolds number, independent of the geometric orientation and void fraction of the bed. Similar measurements were made across the middle layer of each distended bed, and again a single relationship between the corresponding friction factor and the modified Reynolds number was obtained.

Reference: Wentz, Charles A., and George Thodos, **A.I.Ch.E. Journal, 9,** No. 1, p. 81 (January, 1963).

Key Words: Turbulence—6, Mass Transfer-2, Co-axial Jet-5, Mixing-7, Anisotropic-6, Transfer Coefficient-2, Eddy Diffusion-2, Composition-1, Numerical Differentiation-1, Shear-6.

Abstract: Turbulent mass transfer coefficients are calculated as a function of position in regions of developing anisotropic turbulence, with the data of Forstall and Shapiro on co-axial jet mixing. Geometry and relative velocity of the jets are varied. The transfer coefficients thus obtained are related to the patterns of the mean flow by integration along a flow line of the product of a generation rate (proportional to the rate of strain) and a dissipation rate (proportional to the transfer coefficient).

Reference: Howe, N. M., Jr., and C. W. Shipman, **A.I.Ch.E. Journal, 9,** No. 1, p. 85 (January, 1963).

Key Words: Packed Beds-5, Gas-5, Liquid-5, Flow Rate-6, Particle Diameter-6, Bed Length-6, Transport Properties-6, Stagment Film-7, Film Thickness Distribution-7, Mixing-7, Axial Dispersion-8, Mass Transfer-8, Rate Process-9, Transport Phenomena-9, Frequency Response-10, Models-10.

Abstract: A number of experimental investigations of the axial diffusion of mass in packed beds have been reported for both gas and liquid flow systems. The diffusion coefficients of the two systems differ markedly, although previous theoretical analyses (based on the perfect mixing model) indicate that the diffusion coefficient should be independent of the nature of the fluid. It is shown here that the discrepancy arises from a capacitive effect caused by stagnant fluid regions in the packed bed.

Reference: Gottschlich, Chad F., **A.I.Ch.E. Journal, 9,** No. 1, p. 88 (January, 1963).

(*Continued on page 142*)

flux given in reference 2 using orifice equation for single phase outflow with a corrected section $\pi/4\ (2r_o - 1.5\ D_p)^2$.

When larger orifices were used, the outflow gas flow rate increased with the flow rate of fluidizing gas; on the contrary the outflow solid flow rate remained practically constant (Figure 1). The dependence of flow rate of effluxing gas on degree of voids in the column considerably complicates analysis of efflux process. Equations (1) and (2) were derived by supposing a constant degree of voids in the solid-gas system feeding orifice. This assumption is reasonable insofar as flow rates of solid and gas flowing out do not depend on the flow rate of fluidizing gas. With larger orifices outflow gas flow rate definitely depends on distribution of degree of voids upstream orifice, and this in turn depends on the degree of void of the bed, on drag and inertial forces acting on the particles, and on interparticle frictional forces. As expected (2) Equations (1) and (2) cannot be extended to orifices larger than 5 to 7 mm. in diameter, even if an appropriate value of C_D is taken and allowance is made for interparticle friction. Although kinetic energy of solid and gas flowing from orifices is only a limited part (about 20%) of the potential energy of the gas in the bed, a theoretical correlation of data for orifices 7 to 20 mm. in diameter would require more complete expressions for energy balance and drag equations. These should include terms depending on actual distribution of degree of voids upstream orifice. However such a result cannot be reached by considering only gas energy balance and drag equations. Other physical aspects of solid-gas interaction should be considered for a more fundamental approach to the problem.

NOTATION

C_D = drag coefficient, dimensionless
D_p = mean particle diameter, meter
g_c = conversion factor, 9.81 Kg. (meter)/(Kg. force) (sec.^{2})
Q_A = outflow air flow rate, cu. meter/sec.
Q_S = outflow solid flow rate, cu. meter/sec.
r_o = orifice radius, meter
s_p = surface of the particle exposed to the air stream, sq. meter
w_p = volume of the particle, cu. meter
Δp = outflow pressure, mm. water
Φ = shape factor for the Carman-Kozeny correlation, dimensionless
ρ_A = air density, Kg./cu. meter
ρ_p = solid density, Kg./cu. meter

LITERATURE CITED

1. Brown, R. L., and J. C. Richards, *Trans. Inst. Chem. Engrs.*, 38, 243 (1960).
2. Massimilla, Leopoldo, Vittorio Betta, and Carlo Della Rocca, *A.I.Ch.E. Journal*, 7, 502 (1961).
3. Rowe, P. N., and G. A. Henwood, *Trans. Inst. Chem. Engrs.*, 39, 43 (1961).
4. Stockel, I. H., *Chem. Eng. Progr. Symposium Ser. No. 38*, 58, 106 (1962).
5. Vitagliano, G. — Chianese R., Tesi, Università di Napoli, Italia (1961).
6. Zenz, F. A., *Petrol. Refiner*, 41, 159 (1962).

Nonisothermal Velocity Profiles

C. W. GORTON, K. R. PURDY, and C. J. BELL

Georgia Institute of Technology, Atlanta, Georgia

Analytical extensions of the Graetz problem to include the effect of varying viscosity have been made by Cherry (*1*), Yamagata (*4*), and Yang (*5*). The corresponding problem which includes the variation of density for the case of the horizontal tube has so far not been solved analytically.

At present there is no experimental information available on measured velocity profiles for flow through horizontal tubes in which the variation of both density and viscosity is important.

The purpose of the present work was to obtain experimental data on velocity profiles for the flow of mineral oil through a horizontal steam heated tube for Reynolds numbers in the laminar range.

EXPERIMENTAL APPARATUS

The apparatus consisted of a centrifugal pump, venturi meter, air cooling coil, calming chamber, inlet section, test section with steam jacket, probe, cooling coil, and discharge tank. A flow diagram of the apparatus is given in Figure 1.

From the venturi exit the oil entered a finned air-cooled coil which was used to lower the temperature of the oil.

The calming chamber was cylindrical and approximately 6 in. in diameter and 6 ft. long. Several screens were placed in the calming section to help damp out any irregular motions in the oil before it entered the inlet section. The temperature of the oil in the calming section was measured with a copper-constantan thermocouple.

The inlet section and test section were smooth, hard-drawn copper tubing 1.055 in. I.D. and had a wall thickness of approximately 0.010 in. The inlet section was joined to the calming section by means of an 0 ring seal and protruded inside the calming section for a short distance. The inlet section was approximately 10 ft. long and was covered with magnesia insulation. The inlet section and test section were joined with a bakelite connector and 0 ring seals in order to keep the metal inlet and test section tubes from touching each other and thus to simulate a step change in wall temperature at the test section inlet. The test section itself was 10.05 ft. long.

The steam jacket was a 3-in. standard pipe which enclosed the test section and was supplied with low pressure wet steam. The steam temperature was measured with a copper-constantan thermocouple.

A depth gauge micrometer with ± 0.001-in. divisions was used to position the probe. The probe was a total pressure probe and was made of 0.072 in. O.D. hypodermic tubing with a tube wall thickness of 0.0090 in. The static pressure was obtained from a small hole in the test section wall. The difference between the total and the static pressure was read by means of an inverted U-tube manometer with air in the top portion of the manometer. In this way mineral oil at room temperature was used to indicate the difference between the total and static pressure.

Following the probe was a short section of copper tubing connecting the exit of the probe housing with the discharge tank. A coil of copper tubing with water flowing through it was used to cool the oil as it passed through the discharge tank.

From the discharge tank the oil returned to the pump. The discharge tank was located above the pump so that there was always a positive head on the pump.

RESULTS AND DISCUSSION

Tests were run under isothermal conditions to determine the velocity profiles at inlet to the test section. These tests indicated that the inlet profiles were within ± 5% of the corresponding parabolic ones. Runs were made at Reynolds numbers of 650, 950, and 1,325. A maximum value of r/r_o of 0.57 was used in these tests.

Five heated runs were made, and five vertical and three horizontal velocity profiles were taken at the test section exit. The Reynolds number in the test section, based on the inside tube diameter, varied from 850 to 1,400. The corresponding Graetz, Prandtl, and Grashof numbers as well as μ_b/μ_w were essentially the same for all runs. As a consequence the vertical and horizontal velocity profiles were essentially the same for all runs made.

The tube Reynolds number, Prandtl number, Grashof number, and Graetz number were calculated with properties evaluated at the average bulk temperature. The Grashof number was based on tube inside diameter and arithmetic mean temperature difference. The outlet bulk temperature was not measured but was estimated by an energy balance. The specific gravity of the oil used in these experiments and hence the density and the value of β were obtained with a hydrometer. The kinematic viscosity was obtained with a viscometer, and the thermal conductivity was measured in a parallel plate apparatus. The specific heat was not measured but was estimated from data on similar oils. A summary of the property values used is given in Table 1.

As is well known (*2*, *5*) at low probe Reynolds number the pressure coefficient for a square-edged total pressure probe of the type used in these experiments is unity for values of the probe Reynolds number greater than 20, where the probe Reynolds number is based on the outside probe

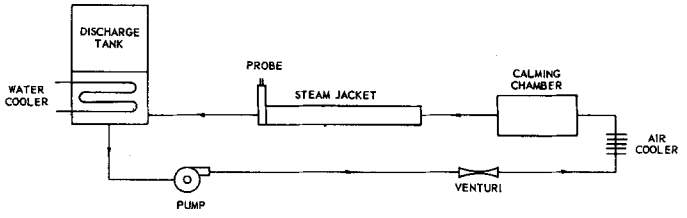

Fig. 1. Schematic of apparatus